JOURNAL OF AGRICULTURAL AND FOOD CHEMISTRY

Article

pubs.acs.org/JAFC

Effect of Silver Nanomaterials on the Activity of Thiol-Containing Antioxidants

Yu-Ting Zhou,[†,‡] Weiwei He,[†,§] Y. Martin Lo,[*,‡] Xiaona Hu,[∥] Xiaochun Wu,[∥] and Jun-Jie Yin[*,†]

[†]Center for Food Safety and Applied Nutrition, U.S. Food and Drug Administration, College Park, Maryland 20740, United States

[‡]Department of Nutrition and Food Science, University of Maryland, College Park, Maryland 20742, United States

[§]Key Laboratory for Micro-Nano Energy Storage and Conversion Materials of Henan Province, Institute of Surface Micro and Nanomaterials, Xuchang University, Xuchang 461000, China

[∥]CAS Key Laboratory of Standardization and Measurement for Nanotechnology, National Center for Nanoscience and Technology, Beijing 100190, China

ABSTRACT: The use of nanomaterials in consumer products is rapidly expanding. In most studies, nanomaterials are examined as isolated ingredients. However, consumer products such as foods, cosmetics, and dietary supplements are complex chemical matrixes. Therefore, interactions between nanomaterials and other components of the product must be investigated to ensure the product's performance and safety. Silver nanomaterials are increasingly being used in food packaging as antimicrobial agents. Thiol-containing compounds, such as reduced glutathione (GSH), cysteine, and dihydrolipoic acid, are used as antioxidants in many consumer products. In the current study, we have investigated the interaction between silver nanomaterials and thiol-containing antioxidants. The selected Ag nanomaterials were Ag coated with citrate, Ag coated with poly(vinylpyrrolidone), and Au nanorods coated with Ag in a core/shell structure. We observed direct quenching of the 1,1-diphenyl-2-picrylhydrazyl radical (DPPH) by all three Ag nanomaterials to varying degrees. The Ag nanomaterials also reduced the quenching of DPPH by GSH to varying degrees. In addition, we determined that the mixture of GSH and Au@Ag nanorods held at 37 °C was less effective at quenching azo radical than at ambient temperature. Furthermore, we determined that Au@Ag nanorods significantly reduced the ability of GSH and cysteine to quench hydroxyl and superoxide radicals. The work presented here demonstrates the importance of examining the chemical interactions between nanomaterials used in products and physiologically important antioxidants.

KEYWORDS: *silver nanomaterials, thiol antioxidant, free radical, ESR, nanosafety*

INTRODUCTION

Reactive oxygen species (ROS), including hydrogen peroxide (H_2O_2), superoxide radical ($O_2^{\bullet-}$), and hydroxyl radical ($^{\bullet}OH$), can damage a variety of cellular targets. Oxidative damage caused by ROS has been implicated in a number of acute and chronic diseases. Antioxidants, such as ascorbic acid and glutathione, are important physiological defenses against oxidative damage. Glutathione, including reduced (GSH) and oxidized (GSSG) forms, is synthesized in all mammalian cells. Glutathione has diverse physiological functions, including detoxification, maintenance of essential thiol status, antioxidant activity, and regulation of growth and death.[1] Dysregulation of GSH synthesis may cause aging[2] and many diseases,[3] e.g., diabetes mellitus,[4] cholestasis,[5] endotoxemia,[6] alcoholic liver disease,[7] and cancer and drug-resistant tumors.[8] Typically, ROS are reduced by cellular GSH, forming GSSG, which is in turn reduced back to GSH by GSH reductase. In this way, GSH can prevent oxidative damage elicited by ROS. A precursor of GSH, the amino acid cysteine, is also believed to play an essential role in reversible redox reactions in cells to limit damage attributable to ROS.[9,10]

Silver usage in medical applications can be traced back for centuries, and current nanotechnology enables more wide and sophisticated applications of nanoscale silver. In many cases, silver nanomaterials are used in food, health care, and consumer products as antimicrobial agents.[11−15] Silver nanoparticles have been found to be broad-spectrum antimicrobials in microorganisms, including *Escherichia coli*, *Staphylococcus aureus*, *E. coli* K12, *Pseudomonas mendocina* KR1, and MS2 bacteriophage,[16−19] as well as several pathogenic fungal species in the genus *Candida*.[20] Because of the increasing use of Ag nanomaterials, there is a need to thoroughly understand their bioactivity and safety under conditions of use. A number of investigators have examined cytotoxicity and genotoxicity resulting from exposure to Ag nanomaterials.[21] We have previously investigated the interaction between Ag nanoparticles and biologically relevant agents and predicted the mechanisms of potential toxicity due to generation of ROS.[22] To fully understand the bioactivity and potential toxicity of Ag nanomaterials, one must consider their interactions with components of biological systems. Because it is well established that Ag nanomaterials participate in redox reactions, it is important to understand the effects of Ag nanomaterials on cellular components involved in redox homeostasis. Antioxidants with sulfhydryl functional groups are among those for consideration. These antioxidants include the endogenous antioxidants glutathione (GSH), cysteine (Cys), and dietary

Received: May 16, 2013
Revised: July 24, 2013
Accepted: July 26, 2013
Published: July 26, 2013

antioxidants dihydrolipoic acid (DHLA) and *N*-acetyl-L-cysteine (NAC).

The results reported by Piao and co-workers[23] suggest that Ag nanoparticles (NPs) can induce generation of ROS, reduce intracellular levels of GSH, and sequentially lead to apoptosis of human liver cells. It has also been reported that, in rat liver cells, exposure to Ag NPs resulted in decreased mitochondrial function accompanied by a reduction in intracellular GSH levels.[24] Reduction in levels of GSH always accompanied the cytotoxicity resulting from exposure to Ag NPs. However, detailed knowledge about the interactions among ROS, GSH, and Ag NPs is lacking. Similar to other thiol-containing antioxidants, NAC has been reported to protect both normal and tumor human cells from cytotoxicity induced by Ag NPs.[25,26] However, the underlying protective mechanism is still unclear.

The strength of the chemical bond between thiol groups and Ag has led to many commercial applications and has important physiological implications. For example, Sellers et al. have examined reactions between thiols and Ag as a method for producing self-assembling monolayers.[27] In addition, the affinity of Ag for thiol groups may be exploited for production of biosensors for detecting cysteine, homocysteine, and GSH.[28,29] Liu et al. have described the importance of interactions between Ag NPs and endogenous thiol-containing compounds during chemical transformations of Ag NP in physiological systems.[30] In their studies dissolution of Ag NPs during digestion to yield Ag^+ played an important role in formation of products between Ag and thiol compounds.

We have investigated the effects of Ag nanomaterials on the antioxidant activity of physiologically and commercially important thiol-containing antioxidants. Antioxidant activity was assessed as the ability to quench radicals. In the present study, we examined quenching of four radicals: DPPH, azo radical, hydroxyl radical, and superoxide radical. Using DPPH, we examined the effects of silver nanoparticles on the scavenging capability of both hydrophilic and lipophilic thiol-containing antioxidants. DPPH was also used to study the temperature dependence for the interaction between silver nanorods and thiol-containing antioxidants. Finally, we examined the effects of silver nanorods on the ability of GSH and cysteine to quench the ROS, superoxide radical, and hydroxyl radical.

MATERIALS AND METHODS

Materials. Silver nanoparticles (50 nm) with a spherical morphology and coated with poly(vinylpyrrolidone) (PVP) or citrate were purchased from nanoComposix, Inc. (San Diego, CA) and used as received. Au@Ag nanorods with cetrimonium bromide (CTAB) (Au nanorods, ∼60 nm in length and ∼15 nm in width; Ag shell, ∼10 nm in thickness) were a gift from Dr. X. C. Wu at the National Center for Nanoscience and Technology, China. The detailed preparation of Au@Ag nanorods was previously described.[31] The spin trap α-(4-pyridyl-1-oxide)-*N*-*tert*-butylnitrone (4-POBN), xanthine, ethanol, phosphate salts (Na_2HPO_4 and NaH_2PO_4), diethylenetriaminepentaacetic acid (DTPA), 1,1-diphenyl-2-picrylhydrazyl radical (DPPH), L-glutathione, reduced (GSH), and L-cysteine (Fluka) were all purchased from Sigma-Aldrich (St. Louis, MO). 2,2′-Azobis[2-(2-imidazolin-2-yl)propane] dihydrochloride (AAPH) was purchased from Wako Chemicals (Richmond, VA). 1-Hydroxy-3-carboxy-2,2,5,5-tetramethylpyrrolidine hydrochloride (CP-H) was obtained from Enzo Life Sciences (Farmingdale, NY). Dihydrolipoic acid (DHLA) was purchased from EMD Millipore (Billerica, MA). The zinc oxide nanoparticle aqueous dispersion (20 wt %, 30−40 nm) was purchased from US Research Nanomaterials, Inc. (Houston, TX). Before use, phosphate buffer was treated with Chelex 100 molecular biology grade resin from Bio-Rad Laboratories (Hercules, CA) to remove trace metal ions. Milli-Q water (18 MΩ cm) was used for all solution preparations.

Characterization. UV−vis spectroscopy was used to characterize changes in nanomaterials during reaction with glutathione. UV−vis absorption spectra were obtained using a Varian Cary 300 spectrophotometer (Santa Clara, CA). Silver nanoparticles coated with PVP (Ag(PVP)) or citrate (Ag(cit)) (0.01 mg/mL) were mixed with 1 mM GSH individually in water, while Au@Ag nanorods (0.1 nM) were diluted in 0.1 mM CTAB to stabilize Ag nanorods and mixed with 1 mM GSH. To monitor the progress of the reaction, absorption spectra were collected at 1 min intervals using the scanning kinetics mode of the spectrophotometer.

Nanomaterials were additionally characterized using transmission electron microscopy (TEM) images, captured on a JEM 2100 FEG (JEOL) transmission electron microscope at an accelerating voltage of 200 kV (located at the NanoCenter, University of Maryland, College Park, MD). To observe the morphological evolution of the nanoparticles before and after incubation with GSH, 0.1 mg/mL Ag NPs and 1 nM Au@Ag nanorods (NRs) were mixed with 10 mM GSH for 10 min and centrifuged (12 000 rpm, 5 min) twice. After the supernatants were decanted, 20 μL of water was added to redisperse the precipitates. The samples for TEM analysis were prepared by adding drops of the redispersed colloidal solutions onto standard holey carbon-coated copper grids, which were then air-dried at room temperature.

DPPH Radical Scavenging Activity. The scavenging activity for DPPH, a stable radical, by antioxidants containing thiol groups was estimated as we previously described.[32] Stock solutions of cysteine (Cys) and reduced glutathione (GSH) were prepared in water. Solutions of dihydrolipoic acid (DHLA) were prepared in ethanol. The control solution contained 0.2 mM DPPH and 10% (20% for DHLA study) (v/v) ethanol in 0.1 mM pH 7.4 phosphate buffer. Ag nanomaterials or each of the three thiol-containing antioxidants were added to DPPH control alone to evaluate their individual scavenging effect on DPPH radical. Then Au@Ag NRs coated with CTAB were preincubated with Cys, GSH, or DHLA at 23 °C for 10 min prior to addition to the DPPH radical control.

To estimate the effect on GSH, three silver nanomaterials were used: Ag(cit), Ag(PVP), and Au@Ag NRs. The Ag NPs and Au@Ag NRs were 0.01 mg/mL and 0.1 nM, respectively. GSH or each of the three silver nanomaterials was added to DPPH control alone to examine their individual reducing effect on DPPH radical. GSH was premixed with different Ag NPs at 23 °C for 10 min prior to addition to the DPPH radical control. ESR spectra were recorded 1 min after mixing DPPH radical with other reagents using the following instrument settings: microwave power, 20 mW; field modulation, 1.5 G; scan range, 100 G. The signal intensity of DPPH radical in sample solutions was normalized to that in the DPPH control solution.

Azo Radical Scavenging Activity. We examined the ability of GSH to scavenge azo radicals in the absence and presence of Au@Ag NRs. Azo radicals were generated by the thermal decomposition of the hydrophilic radical generator AAPH. Scavenging of azo radical was determined by ESR using 4-POBN as the spin trap in PBS (10 mM, pH 7.4). A 20 μM concentration of GSH was premixed with 0.1 nM Ag NRs at 23 or 37 °C for 10 min to study the temperature dependence for the reaction between GSH and Au@Ag NRs. Each sample was then mixed with 50 mM 4-POBN and 10 mM AAPH. Thereafter, the mixture was incubated in a water bath (37 °C) for 10 min to generate azo radicals. ESR spectra were recorded 1 min after sample removal from the water bath. The instrument settings (20 mW microwave power, 1 G field modulation, and 100 G scan range) were used for the present and following ESR experiment.

Hydroxyl Radical (•OH) Scavenging Activity. Hydroxyl radicals were produced by irradiating a zinc oxide nanodispersion with light emitted from a 500 W Xe arc lamp directed through a WG320 filter. This filtered light source emits radiation having wavelengths greater than 350 nm.[33] The yield of •OH was quantified using the spin trap 4-POBN in solution containing ethanol (20%, v/v).[22,34] The final control mixtures contained 0.02 mg/mL ZnO dispersion, 1 mM 4-

POBN, and 20% ethanol (v/v) in 10 mM pH 7.4 phosphate buffer. Au@Ag nanorods were preincubated with GSH or Cys at 37 °C for 10 min prior to photoirradiation of the ZnO control mixture. ESR spectra were recorded 4 min after the initiation of exposure to light.

Superoxide Radical ($O_2^{\bullet -}$) Scavenging Activity. Superoxide radical oxidizes CP-H, which is ESR silent, to a stable nitroxide radical, CP•, that is detectable by ESR spectroscopy.[35] The xanthine−xanthine oxidase system (XAN−XOD) was used to generate the superoxide radical. The final control mixtures contained 1 mM xanthine, 0.1 mM CP-H, 0.1 mM DTPA, and 0.2 U/mL XOD in 10 mM pH 7.4 phosphate buffer. Au@Ag nanorods were preincubated with 10 mM GSH or Cys at 37 °C for 10 min before addition to the control mixture without XOD. Radical generation was initiated by addition of XOD, and the ESR signal was recorded 4 min afterward.

RESULTS AND DISCUSSION

Characterization of Au@Ag Nanorods and Ag Nanoparticles. The UV−vis spectra of noble metal nanoparticles can be used to sensitively monitor their size and aggregation state. This property derives from the surface plasmon resonance (SPR) attributable to these nanoparticles. UV−vis extinction spectra of the silver nanoparticles are illustrated in Figure 1. Both Ag(cit) and Ag(PVP) (50 nm) show an absorption peaked at 420 nm. The nanoparticles were well dispersed due to the protection of coatings that prevent aggregation. When incubated with GSH, the absorption maximum of both Ag NPs gradually decreased in intensity and a second absorption maximum appeared at progressively higher wavelength. The initial reduction rate of the peak at 420 nm of Ag(cit) and Ag(PVP) was 0.26 and 0.17 min^{-1}, respectively. These spectral changes indicate that the silver nanoparticles are aggregating and may be attributed to the formation of a Ag−S bond. However, the maximum adsorption of Ag(cit) diminished faster than that of Ag(PVP). This may be because the neutral PVP coating is not as readily displaced from the surface of Ag NPs as the negatively charged citrate coating. The characteristic SPR peak of in-house-prepared Au@Ag NRs with CTAB was unaffected during incubation for 5 min in the absence of GSH (data not shown, but consistent with a previous report[31]), but the intensity slightly decreased in the presence of GSH. The inconspicuous alteration of the SPR peaks of the nanorods may be a consequence of excessive CTAB, a good positively charged stabilizer.

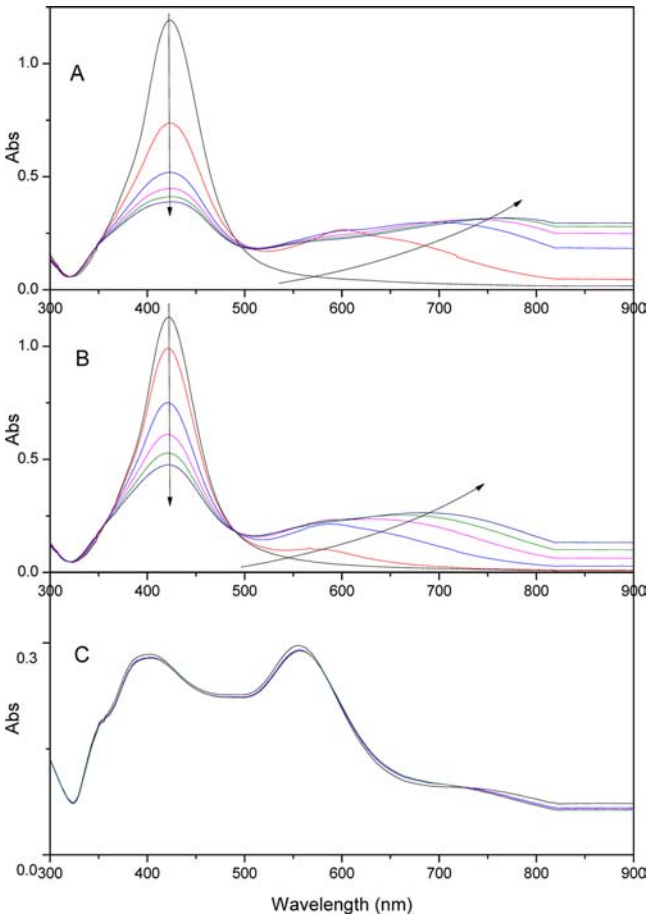

Figure 1. Evolution of UV−vis spectra of Ag nanomaterials incubated with GSH at 23 °C. The spectra were recorded every 1 min for 5 min. Sample solutions included 1 mM GSH and 0.01 mg/mL Ag(cit) NPs (50 nm) (A), Ag(PVP) NPs (50 nm) (B), or 0.1 nM Au@Ag(CTAB) NRs (C). The arrows indicate the direction of the wavelength shift with increasing time.

The morphology of Ag nanorods and nanoparticles is shown in TEM images (Figure 2). The Au@Ag nanorods, which contain a molar ratio of Ag to Au of 0.83, have an orange-slice-like core/shell structure with Au nanorods as a core (~60 in length and ~15 nm in width) and a thick and anisotropic Ag shell with a thickness of ~10 nm (Figure 2A). The detailed method for their preparation was previously described.[31] The morphology and size of Au@Ag nanorods remained the same after reaction with GSH (Figure 2A,A′).The thin-film-like compounds in the TEM image may be solvent residue. The size of the Ag(cit) NPs before and after treatment with GSH was 70.09 ± 6.19 and 64.42 ± 7.62 nm, respectively (Figure 2B,B′). The slight shrinkage of silver nanoparticles indicates dissolution of Ag(cit) NPs. Since silver is vulnerable to oxidation in oxygenated media, silver ions (Ag^+) are possibly accumulated on the surface of silver nanoparticles. It is noticeable that, after reaction with GSH, products having a cross-linked structure appeared. These cross-linked structures may be silver sulfide complexes formed from superficial Ag^+ and GSH. In contrast to changes observed with Ag(cit) NPs, the size of Ag(PVP) NPs was 65.60 ± 8.85 and 66.9 ± 6.16 nm before and after mixing with GSH, respectively (Figure 2C,C′). The particle morphology remained the same as well. This observation is consistent with previous reports that the dissolution of Ag NPs coated with citrate is faster than that for Ag NPs coated with PVP.[36]

DPPH Radical Scavenging Activity. In many applications, to estimate the antioxidant capacity of food or their extracts, the stable nitrogen-centered radical DPPH has been used.[37] The assay has been generally accepted as a simple and sensitive method in antioxidant studies.[38] DPPH radical is ESR detectable with a one-line spectrum, as shown in the inset to Figure 3. When the DPPH radical accepts one H atom from antioxidants, it becomes ESR silent. In Figure 3, the ESR signal intensity from each sample solution was normalized to that from the control solution and expressed as a percentage; thus, the antioxidant ability is inversely proportional to the normalized signal intensity. Three thiol-containing antioxidants, Cys, GSH, and DHLA, all quenched DPPH radical to various extents (Figure 3, red). Also, we found that Au@Ag NRs can scavenge DPPH radical (Figure 3, blue), though only slightly. When preincubated with Ag NRs, the scavenging ability of the three antioxidants was reduced (Figure 3, green).

The reduced scavenging ability of the antioxidants may be caused by the replacement of functional −SH with −AgS, which is formed through partially electrostatic and partially

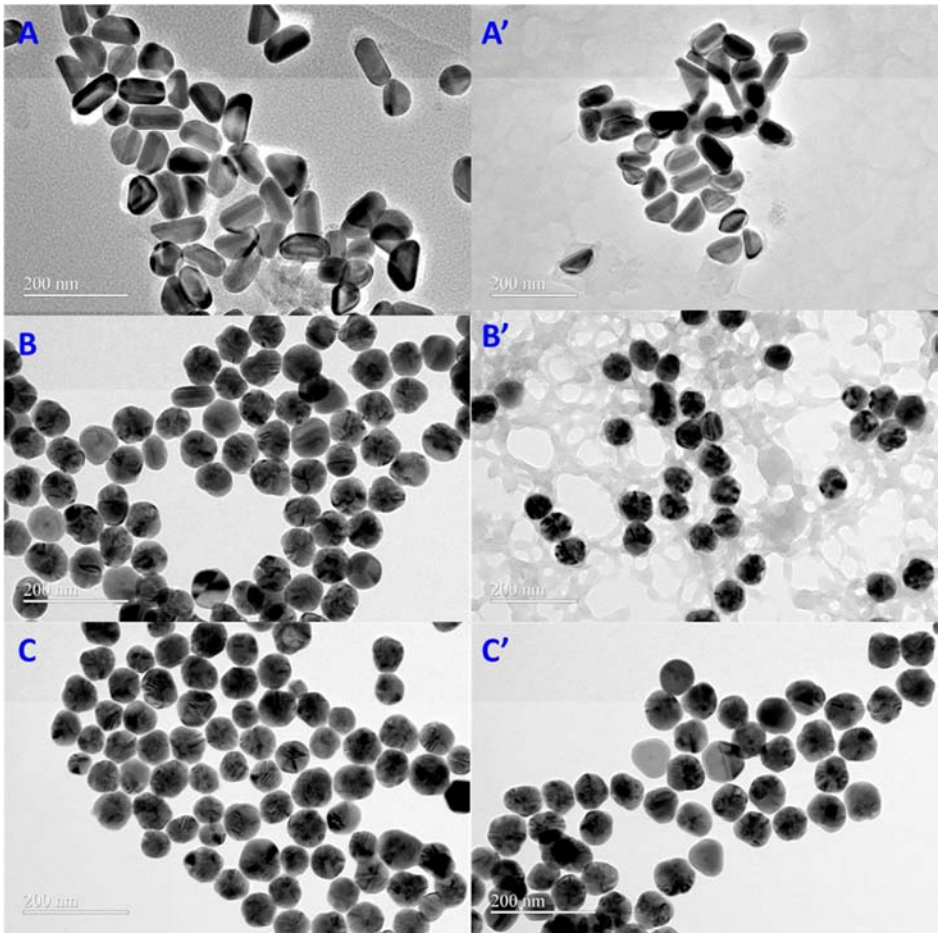

Figure 2. TEM images of Au@Ag nanorods (A) and Ag NPs coated with citrate (B) and PVP (C) before (A–C) and after (A′–C′) incubation with GSH at 23 °C for 10 min.

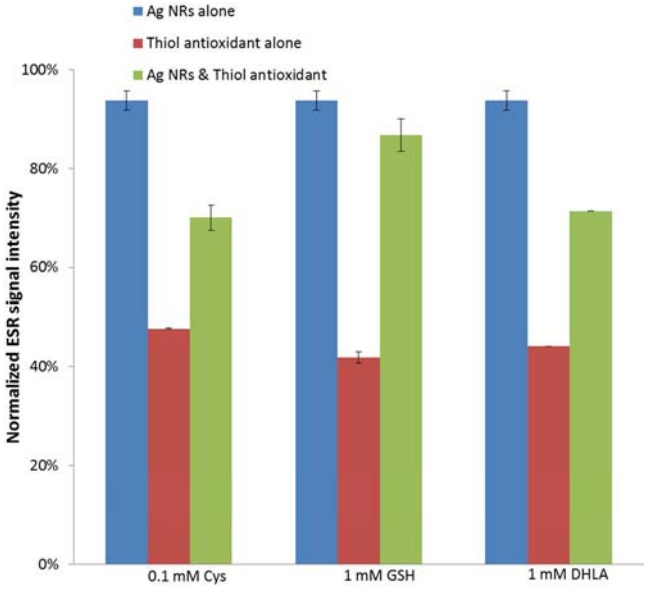

Figure 3. DPPH scavenging effect for different thiol-containing hydrophilic and lipophilic antioxidants influenced by 0.1 nM Au@Ag(CTAB) NRs. The DPPH signal intensity of each sample was normalized to that of the DPPH control. The inset shows the ESR spectrum of the DPPH radical.

covalent binding.[39] It has been previously found that biothiols, e.g., homocysteine, cysteine, and glutathione, were absorbed to the surface of Ag NPs via a conjugated Ag–S bond.[40] Sulfide complexation of Ag NPs also occurred with the formation Ag_2S or precipitate, and the surface of Ag NPs (oxidized to Ag^+) reacted with sulfide anions, producing Ag_xS_y.[41]

In the same range of concentration, the scavenging ability of DHLA was similar to that of GSH. However, after incubation with Au@Ag NRs, the scavenging ability of DHLA was less affected than the scavenging ability of GSH. This indicates a less efficient binding of Ag NRs to DHLA than to GSH, which may be attributed to the more bulky structure of DHLA and thus ineffective interfacial contact of DHLA with Ag NRs.

Both commercial Ag NPs and the Au@Ag NRs prepared in-house were used to examine their inhibitory effect on the DPPH radical scavenging activity of GSH, an important endogenous antioxidant containing thiol. Direct quenching of the DPPH radical by Ag NPs was observed. Citrate-coated Ag NPs quenched the DPPH radical to a greater extent than PVP-coated Ag NPs (Figure 4, blue). Significant quenching of DPPH was seen in the presence of GSH (Figure 4, red). When GSH was preincubated with the Ag nanomaterials, the quenching activity of GSH toward DPPH was diminished to varying degrees (Au@Ag NRs > Ag NPs coated with citrate > Ag NPs coated with PVP). The results suggest a greater affinity of GSH for citrate-coated Ag NPs than PVP-coated Ag NPs. The result is in agreement with the previous finding that GSH

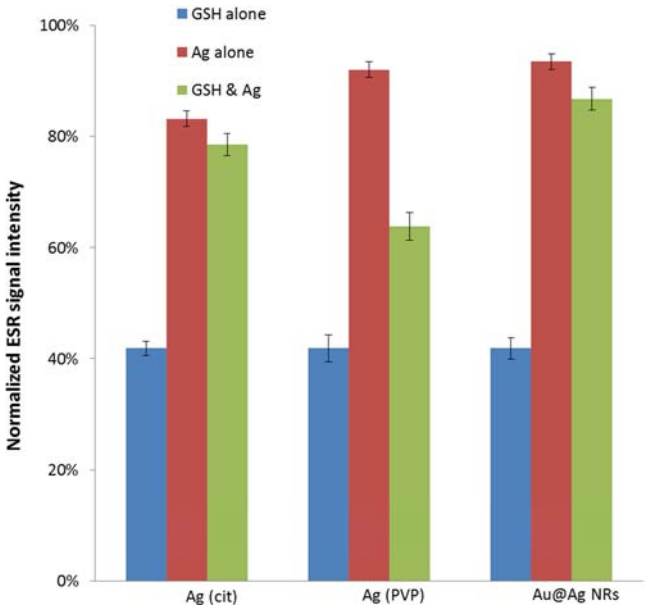

Figure 4. Effect of Ag nanomaterials on DPPH radical scavenging by 1 mM GSH. Ag nanomaterials, including 0.01 mg/mL Ag NPs, coated with citrate or PVP, and 0.1 nM Au@Ag NRs, were preincubated with GSH. The control sample included 0.2 mM DPPH and 10% ethanol in 10 mM pH 7.4 phosphate buffer. The DPPH signal intensity of each sample was normalized to that of the DPPH control.

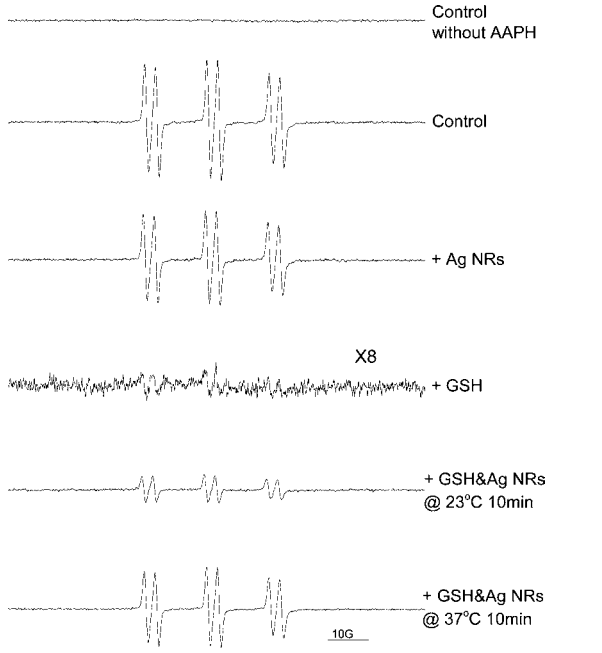

Figure 5. AAPH radical scavenging effect of 1 mM GSH impacted by 0.1 nM Au@Ag NRs. The control sample contained 10 mM AAPH and 50 mM 4-POBN in 10 mM pH 7.4 phosphate buffer.

induces more rapid aggregation of Ag NPs with citrate (Figure 1). Among them, preincubation of GSH with the Au@Ag NRs had the most effect on GSH's ability to quench DPPH. This indicates that the Ag layers in an orange-slice-like shape partially deactivate GSH due to the formation of a Ag−S bond.

Azo Radical Scavenging Activity. AAPH is a hydrophilic radical generator widely used as an inducer of lipid peroxidation in many in vitro assays for determining antioxidant activity.[42−44] AAPH undergoes thermal decomposition to generate azo radicals, which can be trapped by 4-POBN to form the spin adduct 4-POBN/$^{\bullet}$A.[45] In the presence of 10 mM AAPH, AAPH-derived radicals were detected in the form of 4-POBN/$^{\bullet}$A with hyperfine splitting parameters of a_N = 14.92 G and a_H = 2.57 G, observed as a six-line spectrum (Figure 5), similar to previous reports.[45] With the addition of Au@Ag NRs, the intensity of the characteristic signal was slightly reduced, while 1 mM GSH nearly eliminated the signal for the spin adduct. The interaction between the Au@Ag NRs and GSH, and effects on scavenging azo radicals generated by AAPH, was investigated at 23 °C and at a physiologically relevant temperature, 37 °C. As seen clearly in spectra 5 and 6 of Figure 5, premixing of Au@Ag NRs at both temperatures reduced scavenging of azo radicals by GSH. This reduction in GSH's scavenging activity was more pronounced at the higher temperature. This indicates that GSH was more vulnerable to adsorb on Ag NRs and thus to form a Ag−S bond at elevated temperature. Therefore, less GSH was available in electron donation from its thiol group to azo radical.

Hydroxyl Radical Scavenging Activity. As the most reactive ROS, hydroxyl radicals ($^{\bullet}$OH) are an excellent indicator to estimate the antioxidant property of a target compound. Because of the reactivity of the hydroxyl radical, we utilized a double spin trapping system, in which the radical product from $^{\bullet}$OH and a $^{\bullet}$OH scavenger, usually an organic solvent such as ethanol, is trapped by a nitrone-based spin trap.[34] In the current study, hydroxyl radicals were generated by irradiating an aqueous suspension of ZnO. The hydroxyl radicals then reacted with ethanol followed by the formation of spin adduct 4-POBN/$^{\bullet}$CH(OH)CH$_3$. This spin adduct has a characteristic six-line ESR spectrum with splitting parameters of a_N = 15.58 and a_H = 2.60. The introduction of Au@Ag NRs alone only slightly changed the shape and amplitude of the ESR signal expected for the 4-POBN/$^{\bullet}$CH(OH)CH$_3$ spin adduct (Figure 6, spectra 1 and 2). Antioxidants cysteine and GSH had comparable power in reducing the production of the hydroxyl radical (Figure 6, spectra 3 and 5). Thiol-containing antioxidants quench the hydroxyl radical by donation of one electron or H atom from the sulfhydryl group to the hydroxyl radical with concomitant formation of a relatively unreactive thiyl radical, which cannot be trapped by 4-POBN. After premixing at a biologically relevant temperature, Au@Ag NRs influenced the ability of both GSH and cysteine to react with hydroxyl radicals to different degrees. The scavenging capability of cysteine was almost completely diminished (Figure 6, spectrum 6), while a substantial amount of scavenging remained for GSH (Figure 6, spectrum 4). This may be caused by the structure of GSH, which may have placed steric limitations on its interaction with Au@Ag NRs compared to cysteine.

Superoxide Radical Scavenging Activity. $O_2^{\bullet-}$ is another physiologically important ROS which is continuously generated in cells. The endogenous antioxidant enzyme superoxide dismutase (SOD) is a critical part of the cellular defense against superoxide radical. As with other radicals, superoxide radicals can be trapped by ESR-silent spin probes such as DMPO and BMPO to form stable nitroxide radicals DMPO/$^{\bullet}$OH and BMPO/$^{\bullet}$OOH, respectively. In addition, superoxide can oxidize CP-H to CP$^{\bullet}$, which may be identified and quantified by ESR. However, the reaction rate of superoxide radical with CP-H is significantly higher than that of other spin traps.[35,46] Therefore, CP-H may be used at lower

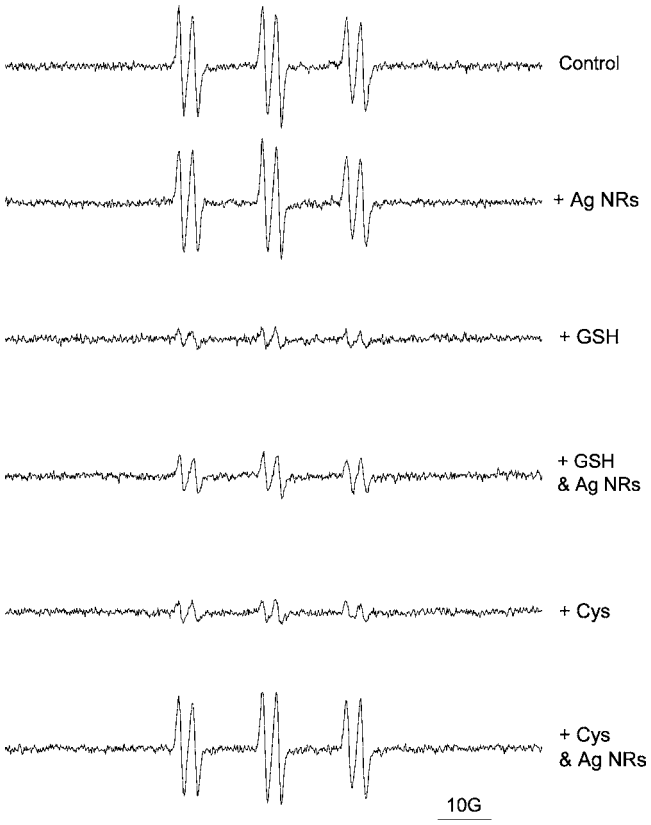

Figure 6. Hydroxyl radical scavenging effect of 10 mM Cys and GSH affected by 1 nM Au@Ag NRs. The control sample consisted of 0.02 mg/mL ZnO dispersion, 1 mM 4-POBN, and 20% ethanol in 10 mM pH 7.4 phosphate buffer.

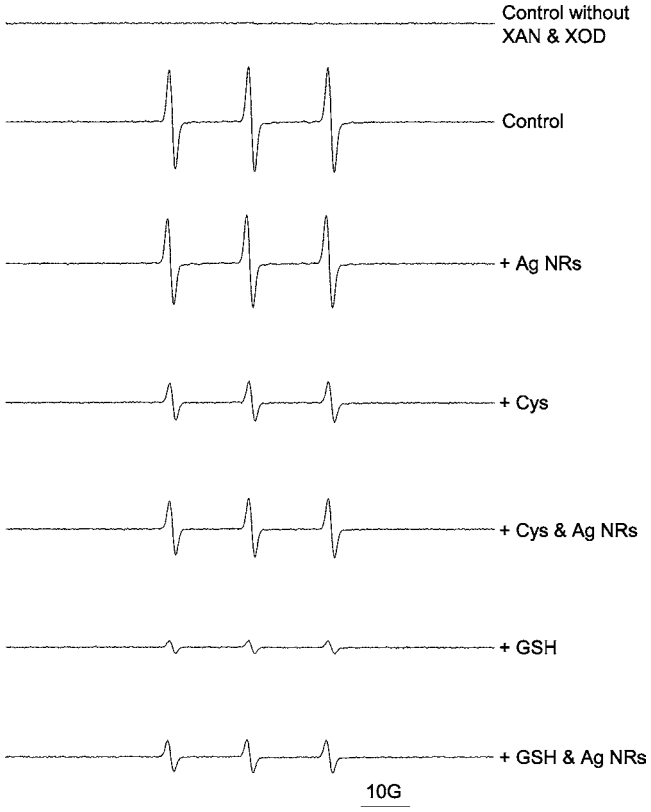

Figure 7. Superoxide radical scavenging effect of 10 mM cysteine and GSH influenced by 1 nM Au@Ag NRs. The control solution contained 1 mM xanthine, 0.1 mM DTPA, 0.1 mM CP-H, and 0.2 U/mL XOD in 10 mM pH 7.4 phosphate buffer.

concentrations for trapping the superoxide radical, avoiding artifacts due to the introduction of spin probes. The xanthine/xanthine oxidase system was employed to generate a superoxide radical, which in turn abstracts a H atom from CP-H to form $CP^{\bullet}$. The ESR spectrum of $CP^{\bullet}$ consists of a three-line spectrum with hyperfine splitting constant a_N = 16.2 G (Figure 7). Au@Ag NRs had a negligible effect on the production of superoxide radical (Figure 7, spectra 2 and 3), but both cysteine and GSH showed strong quenching activity on the radicals (Figure 7, spectra 4 and 6). It has been previously described by Dikalov et al. that nitroxyl radicals, $CP^{\bullet}$, can be reduced to CP-H by the antioxidants GSH, cysteine, and ascorbate.[35] Preincubation of cysteine and GSH with Ag NRs resulted in a partially decreased scavenging ability of the two antioxidants against superoxide radical (Figure 7, spectra 5 and 7).

Using the DPPH radical generation system, all three Ag nanomaterials, Ag(cit), Ag(PVP), and Au@Ag nanorods, reduced the quenching of DPPH radical by GSH to varying degrees (Ag(cit), Au@Ag nanorods > Ag(PVP)). We also observed that Au@Ag nanorods reduced the quenching of DPPH by any of the three antioxidants: GSH, cysteine, and dihydrolipoic acid. This may be attributed to the formation of Ag−S, which diminished the reducing ability of the sulfhydryl group. In addition, we examined the temperature dependence for effects of Au@Ag nanorods on GSH using azo radicals. The effect of Au@Ag nanorods on scavenging the azo radical was greater at physiological temperature than at room temperature. This would be expected as a result of an accelerated reaction between the sulfhydryl group and Ag NPs at higher temperature. Moreover, Au@Ag nanorods significantly reduced the ability of the hydrophilic endogenous antioxidants GSH and cysteine to quench hydroxyl and superoxide radicals.

Many previous studies indicate that the toxicity induced by Ag NPs involves oxidative stress or ROS.[23,24] Our study directly investigates the effect of Ag nanomaterials on individual free radicals and their potential role in weakening the capability of biologically important and dietary antioxidants. This suggests that Ag nanomaterials may cause oxidative stress by jeopardizing either endogenous or dietary antioxidant defense. The work presented here demonstrates the importance of examining the chemical interactions between nanomaterials used in products and physiologically important antioxidants.

AUTHOR INFORMATION

Corresponding Author

*Phone: 240-402-1991. Fax: 201-436-2624. E-mail: junjie.yin@fda.hhs.gov (J.-J.Y.); ymlo@umd.edu (Y.M.L.).

Funding

This work was partially supported by a regulatory science grant under the U.S. Food and Drug Administration (FDA) Nanotechnology CORES Program and by the Office of Cosmetics and Colors, Center for Food Safety and Applied Nutrition (CFSAN)/FDA (Y.-T.Z., W.H., and J.-J.Y.). We acknowledge the support of the Maryland NanoCenter and its NispLab. The NispLab is supported in part by the National Science Foundation (NSF) as a Materials Research Science and Engineering Center (MRSEC) shared experimental facility.

Notes

The authors declare no competing financial interest.

■ ACKNOWLEDGMENTS

We thank Wayne Wamer (Center for Food Safety and Applied Nutrition, U.S. Food and Drug Administration, CFSAN/FDA) for his valuable discussion and comments. This article is not an official U.S. FDA guidance or policy statement. No official support or endorsement by the U.S. FDA is intended or should be inferred.

■ ABBREVIATIONS

GSH, reduced glutathione; GSSG, oxidized glutathione; ESR, electron spin resonance; ROS, reactive oxygen species; H_2O_2, hydrogen peroxide; OH, hydroxyl radical; $O_2^{\bullet-}$, superoxide radical; DHLA, dihydrolipoic acid; Cys, cysteine; Ag NPs, silver nanoparticles; Ag NRs, silver nanorods; PVP, poly(vinylpyrrolidone); DPPH, 1,1-diphenyl-2-picrylhydrazyl radical; CTAB, cetrimonium bromide; 4-POBN, α-(4-pyridyl-1-oxide)-*N*-*tert*-butylnitrone; DTPA, diethylenetriaminepentaacetic acid; AAPH, 2,2′-azobis[2-(2-imidazolin-2-yl)propane] dihydrochloride; CP-H, 1-hydroxy-3-carboxy-2,2,5,5-tetramethylpyrrolidine hydrochloride; XOD, xanthine oxidase

■ REFERENCES

(1) Lu, S. C. Regulation of glutathione synthesis. *Mol. Aspects Med.* **2009**, *30*, 42−59.
(2) Wang, H.; Liu, H.; Liu, R.-M. Gender difference in glutathione metabolism during aging in mice. *Exp. Gerontol.* **2003**, *38*, 507−517.
(3) Townsend, D. M.; Tew, K. D.; Tapiero, H. The importance of glutathione in human disease. *Biomed. Pharmacother.* **2003**, *57*, 145−155.
(4) Okouchi, M.; Okayama, N.; Alexander, J. S.; Aw, T. Y. NRF2-dependent glutamate-L-cysteine ligase catalytic subunit expression mediates insulin protection against hyperglycemia-induced brain endothelial cell apoptosis. *Curr. Neurovasc. Res.* **2006**, *3*, 249−261.
(5) Tan, K. P.; Yang, M.; Ito, S. Activation of nuclear factor (erythroid-2 like) factor 2 by toxic bile acids provokes adaptive defense responses to enhance cell survival at the emergence of oxidative stress. *Mol. Pharmacol.* **2007**, *72*, 1380−1390.
(6) Zhang, C. J.; Walker, L. M.; Hinson, J. A.; Mayeux, P. R. Oxidant stress in rat liver after lipopolysaccharide administration: Effect of inducible nitric-oxide synthase inhibition. *J. Pharmacol. Exp. Ther.* **2000**, *293*, 968−972.
(7) Lee, T. D.; Sadda, M. R.; Mendler, M. H.; Bottiglieri, T.; Kanel, G.; Mato, J. M.; Lu, S. C. Abnormal hepatic methionine and glutathione metabolism in patients with alcoholic hepatitis. *Alcohol.: Clin. Exp. Res.* **2004**, *28*, 173−181.
(8) Lu, S. C. Regulation of hepatic glutathione synthesis: Current concepts and controversies. *FASEB J.* **1999**, *13*, 1169−1183.
(9) Ball, R. O.; Courtney-Martin, G.; Pencharz, P. B. The in vivo sparing of methionine by cysteine in sulfur amino acid requirements in animal models and adult humans. *J. Nutr.* **2006**, *136*, 1682S−1693S.
(10) Wlodek, L. Beneficial and harmful effects of thiols. *Pol. J. Pharmacol.* **2002**, *54*, 215−223.
(11) Maillard, J.-Y.; Hartemann, P. Silver as an antimicrobial: Facts and gaps in knowledge. *Crit. Rev. Microbiol.* **2012**, Early Online, 1−11.
(12) Geranio, L.; Heuberger, M.; Nowack, B. The behavior of silver nanotextiles during washing. *Environ. Sci. Technol.* **2009**, *43*, 8113−8118.
(13) Wilkinson, L. J.; White, R. J.; Chipman, J. K. Silver and nanoparticles of silver in wound dressings: A review of efficacy and safety. *J. Wound Care* **2011**, *20*, 543−549.
(14) Nobile, M. A. d.; Cannarsi, M.; Altieri, C.; Sinigaglia, M.; Favia, P.; Iacoviello, G.; D'Agostino, R. Effect of Ag-containing nanocomposite active packaging system on survival of *Alicyclobacillus acidoterrestris*. *J. Food Sci.* **2004**, *69*, E379−E383.
(15) Benn, T. M.; Westerhoff, P. Nanoparticle silver released into water from commercially available sock fabrics. *Environ. Sci. Technol.* **2008**, *42*, 4133−4139.
(16) da Silva Paula, M. M.; Franco, C. V.; Baldin, M. C.; Rodrigues, L.; Barichello, T.; Savi, G. D.; Bellato, L. F.; Fiori, M. A.; da Silva, L. Synthesis, characterization and antibacterial activity studies of poly-{styrene-acrylic acid} with silver nanoparticles. *Mater. Sci. Eng., C* **2009**, *29*, 647−650.
(17) Cho, K. H.; Park, J. E.; Osaka, T.; Park, S. G. The study of antimicrobial activity and preservative effects of nanosilver ingredient. *Electrochim. Acta* **2005**, *51*, 956−960.
(18) Lee, B. U.; Yun, S. H.; Ji, J.-H.; Bae, G.-N. Inactivation of *S. epidermidis*, *B. subtilis*, and *E. coli* bacteria bioaerosols deposited on a filter utilizing airborne silver nanoparticles. *J. Microbiol. Biotechnol.* **2008**, *18*, 176−182.
(19) Zodrow, K.; Brunet, L.; Mahendra, S.; Li, D.; Zhang, A.; Li, Q.; Alvarez, P. J. J. Polysulfone ultrafiltration membranes impregnated with silver nanoparticles show improved biofouling resistance and virus removal. *Water Res.* **2009**, *43*, 715−723.
(20) Panacek, A.; Kolar, M.; Vecerova, R.; Prucek, R.; Soukupova, J.; Krystof, V.; Hamal, P.; Zboril, R.; Kvitek, L. Antifungal activity of silver nanoparticles against *Candida* spp. *Biomaterials* **2009**, *30*, 6333−6340.
(21) de Lima, R.; Seabra, A. B.; Duran, N. Silver nanoparticles: A brief review of cytotoxicity and genotoxicity of chemically and biogenically synthesized nanoparticles. *J. Appl. Toxicol.* **2012**, *32*, 867−879.
(22) He, W. W.; Zhou, Y. T.; Wamer, W. G.; Boudreau, M. D.; Yin, J. J. Mechanisms of the pH dependent generation of hydroxyl radicals and oxygen induced by Ag nanoparticles. *Biomaterials* **2012**, *33*, 7547−7555.
(23) Piao, M. J.; Kang, K. A.; Lee, I. K.; Kim, H. S.; Kim, S.; Choi, J. Y.; Choi, J.; Hyun, J. W. Silver nanoparticles induce oxidative cell damage in human liver cells through inhibition of reduced glutathione and induction of mitochondria-involved apoptosis. *Toxicol. Lett.* **2011**, *201*, 92−100.
(24) Hussain, S. M.; Hess, K. L.; Gearhart, J. M.; Geiss, K. T.; Schlager, J. J. In vitro toxicity of nanoparticles in BRL 3A rat liver cells. *Toxicol. Vitro* **2005**, *19*, 975−983.
(25) Chairuangkitti, P.; Lawanprasert, S.; Roytrakul, S.; Aueviriyavit, S.; Phummiratch, D.; Kulthong, K.; Chanvorachote, P.; Maniratanachote, R. Silver nanoparticles induce toxicity in A549 cells via ROS-dependent and ROS-independent pathways. *Toxicol. Vitro* **2013**, *27*, 330−338.
(26) Funez, A. A.; Haza, A. I.; Mateo, D.; Morales, P. *In vitro* evaluation of silver nanoparticles on human tumoral and normal cells. *Toxicol. Mech. Methods* **2013**, *23*, 153−160.
(27) Sellers, H.; Ulman, A.; Shnidman, Y.; Eilers, J. E. Structure and binding of alkanethiolates on gold and silver surfaces: Implications for self-assembled monolayers. *J. Am. Chem. Soc.* **1993**, *115*, 9389−9401.
(28) Yuan, X.; Tay, Y.; Dou, X.; Luo, Z.; Leong, D. T.; Xie, J. Glutathione-protected silver nanoclusters as cysteine-selective fluorometric and colorimetric probe. *Anal. Chem.* **2012**, *85*, 1913−1919.
(29) Zhang, N.; Qu, F.; Luo, H. Q.; Li, N. B. Sensitive and selective detection of biothiols based on target-induced agglomeration of silvernanoclusters. *Biosens. Bioelectron.* **2013**, *42*, 214−218.
(30) Liu, J. Y.; Wang, Z. Y.; Liu, F. D.; Kane, A. B.; Hurt, R. H. Chemical transformations of nanosilver in biological environments. *ACS Nano* **2012**, *6*, 9887−9899.
(31) Xiang, Y. U.; Wu, X. C.; Liu, D. F.; Li, Z. Y.; Chu, W. G.; Feng, L. L.; Zhang, K.; Zhou, W. Y.; Xie, S. S. Gold nanorod-seeded growth of silver nanostructures: From homogeneous coating to anisotropic coating. *Langmuir* **2008**, *24*, 3465−3470.
(32) Zhou, Y. T.; He, W.; Wamer, W. G.; Hu, X.; Wu, X.; Lo, Y. M.; Yin, J. J. Enzyme-mimetic effects of gold@platinum nanorods on the antioxidant activity of ascorbic acid. *Nanoscale* **2013**, *5*, 1583−1591.
(33) Jaeger, C. D.; Bard, A. J. Spin trapping and electron spin resonance detection of radical intermediates in the photodecomposi-

tion of water at titanium dioxide particulate systems. *J. Phys. Chem.* **1979**, *83*, 3146−3152.
(34) Gunther, M. R.; Hanna, P. M.; Mason, R. P.; Cohen, M. S. Hydroxyl radical formation from cuprous ion and hydrogen-peroxide: A spin-trapping study. *Arch. Biochem. Biophys.* **1995**, *316*, 515−522.
(35) Dikalov, S.; Skatchkov, M.; Bassenge, E. Spin trapping of superoxide radicals and peroxynitrite by 1-hydroxy-3-carboxy-pyrrolidine and 1-hydroxy-2,2,6,6-tetramethyl-4-oxo-piperidine and the stability of corresponding nitroxyl radicals towards biological reductants. *Biochem. Biophys. Res. Commun.* **1997**, *231*, 701−704.
(36) Gondikas, A. P.; Morris, A.; Reinsch, B. C.; Marinakos, S. M.; Lowry, G. V.; Hsu-Kim, H. Cysteine-induced modification of zero-valent silver nanomaterials: Implications for particle surface chemistry, aggregation, dissolution, and silver speciation. *Environ. Sci. Technol.* **2012**, *46*, 7037−7045.
(37) Molyneux, P. The use of the stable free radical diphenylpicrylhydrazyl (DPPH) for estimating antioxidant activity. *J. Sci. Technol.* **2004**, *26*, 211−219.
(38) Moon, J. K.; Shibamoto, T. Antioxidant assays for plant and food components. *J. Agric. Food Chem.* **2009**, *57*, 1655−1666.
(39) Pakiari, A. H.; Jamshidi, Z. Nature and strength of M−S Bonds (M = Au, Ag, and Cu) in binary alloy gold clusters. *J. Phys. Chem. A* **2010**, *114*, 9212−9221.
(40) Chen, Z.; He, Y. J.; Luo, S. L.; Lin, H. L.; Chen, Y. F.; Sheng, P. T.; Li, J. X.; Chen, B. B.; Liu, C. B.; Cai, Q. Y. Label-free colorimetric assay for biological thiols based on ssDNA/silver nanoparticle system by salt amplification. *Analyst* **2010**, *135*, 1066−1069.
(41) Choi, O.; Cleuenger, T. E.; Deng, B.; Surampalli, R. Y.; Ross, L., Jr.; Hu, Z. Role of sulfide and ligand strength in controlling nanosilver toxicity. *Water Res.* **2009**, *43*, 1879−1886.
(42) Cetojevic-Simin, D. D.; Canadanovic-Brunet, J. M.; Bogdanovic, G. M.; Djilas, S. M.; Cetkovic, G. S.; Tumbas, V. T.; Stojiljkovic, B. T. Antioxidative and antiproliferative activities of different horsetail (*Equisetum arvense* L.) extracts. *J. Med. Food* **2010**, *13*, 452−459.
(43) Freyaldenhoven, M. A.; Lehman, P. A.; Franz, T. J.; Lloyd, R. V.; Samokyszyn, V. M. Retinoic acid-dependent stimulation of 2,2′-azobis(2-amidinopropane)-initiated autoxidation of linoleic acid in sodium dodecyl sulfate micelles: A novel prooxidant effect of retinoic acid. *Chem. Res. Toxicol.* **1998**, *11*, 102−110.
(44) Dikalov, S.; Losik, T.; Arbiser, J. L. Honokiol is a potent scavenger of superoxide and peroxyl radicals. *Biochem. Pharmacol.* **2008**, *76*, 589−596.
(45) Sagrista, M. L.; Garcia, A. F.; De Madariaga, M. A.; Mora, M. Antioxidant and pro-oxidant effect of the thiolic compounds N-acetyl-L-cysteine and glutathione against free radical-induced lipid peroxidation. *Free Radical Res.* **2002**, *36*, 329−340.
(46) Dikalov, S.; Skatchkov, M.; Fink, B.; Bassenge, E. Quantification of superoxide radicals and peroxynitrite in vascular cells using oxidation of sterically hindered hydroxylamines and electron spin resonance. *Nitric Oxide* **1997**, *1*, 423−431.